Quantification of Rock Breakdown for Experimental Weathering Studies

Dawn T. Nicholson

School of Earth Sciences, University of Leeds, Leeds, West Yorkshire, LS2 9JT, United Kingdom.
E-mail: dawn@earth.leeds.ac.uk; Tel: +44 (0)113 233 5234; Fax: +44 (0)113 233 5259.

ABSTRACT

Determination of the severity of rock breakdown due to experimental weathering is strongly influenced by the properties quantified. Traditionally, percentage weight loss has been used to quantify breakdown but this method does not reflect in situ breakdown, nor hidden, internal breakdown which may occur at the microscale. In this paper, results of some experimental rock weathering studies are presented to illustrate the relative merits associated with a range of different methods for quantifying rock breakdown. A range of sedimentary rocks were subjected to accelerated freezing and thawing, salt weathering and wetting and drying tests. The amount of deterioration was measured using techniques selected to provide insight into different facets of rock breakdown. For instance, percentage weight loss was measured to indicate the extent of material detachment; change in fracture density was measured to indicate visible, *in situ* weakening and fracturing; and fracture porosity (based on change in ultrasonic velocity) was calculated to indicate change in void space induced by weathering. Percentage change in Young's dynamic modulus was also recorded to indicate changes in elastic and mechanical properties.

The results show that in some cases there is good agreement between different methods, in terms of the relative magnitude of breakdown and temporal trends, while in other cases there is little or

no agreement. For cases in which there is good agreement between methods, it can be inferred that a range of breakdown processes are operating and that the quantification of breakdown is therefore independent of the method used. However, the converse is true for rocks where there is poor agreement between methods. For these, it can be inferred that a much narrower range of breakdown processes are operating and that the results of quantification of breakdown are therefore dependent on the method used. This may bring into question the validity of breakdown assessments for some rocks where the results are based on a single measurement method.

The paper includes a description of the theoretical basis of the measurement methods listed. Selected results from experimental weathering are used to illustrate their relative merits. It is concluded that rock weathering studies would benefit from a more holistic approach to the quantification of breakdown which utilises several complementary indicators.

INTRODUCTION

Experimental rock weathering studies are usually designed (i) to simulate the natural weathering environment to a greater or lesser extent, (ii) to induce breakdown, and (iii) to test hypotheses. The primary advantage of conducting experimental rock weathering is that the relative susceptibility of rocks, the mode of breakdown, the nature of weathering processes and the role of rock properties can be observed in a comparatively controlled environment. There is an increasing trend to monitoring changes in rock properties caused by experimental weathering. For example, some authors have monitored changes in pore properties (eg Tugrul 1997; Nicholson 2001) while others have monitored changes in mechanical properties such as rock strength (Torok et al 2000). This is a welcome development, but it is also important that quantification of

the *amount* of breakdown occurring is not neglected. The amount of breakdown is a measure of the susceptibility of a rock to the experimental conditions to which it is subject. Traditionally, the amount of breakdown has been measured by recording the percentage weight loss (eg Goudie 1974; Swantesson 1985; Jerwood et al 1990a and b). This has limitations, because, although it enables quantification of the extent of material detachment, it does not reflect in situ breakdown or hidden deterioration. This means that rocks in which breakdown is dominated by mechanisms other than detachment of fragments or grains could be considered more resistant to weathering than they actually are. Alternate methods have been used to quantify breakdown in geomorphic studies such as the use of ultrasonic velocity (eg Fahey and Gowan 1979; Allison 1988, 1990; Murphy and Inkpen 1996; Goudie 1999). However, there remains a heavy reliance on percentage weight loss for quantification of rock breakdown for many testing *standards* such as those prescribed by the A.S.T.M. (American Society for Testing Materials), B.S.I. (British Standards Institution) and various European agencies. In this paper several methods for quantifying rock breakdown are described. Their relative merits are discussed with reference to results from some experimental weathering tests conducted on a range of sedimentary rocks.

EXPERIMENTAL WEATHERING DESIGN

Cylindrical samples of a variety of arenaceous and calcareous sedimentary rocks were subjected to experimental freeze-thaw, wetting and drying and salt weathering as described in Nicholson (2000, 2001). The rocks used in testing comprised two chalks of contrasting density; dolomitic, sparry and oolitic limestones; micaceous, calcareous and muddy sandstones; a metasediment and a siltstone. These are described in detail in Nicholson and Nicholson (2000).

INDICATORS OF DETERIORATION

The amount of rock breakdown induced by experimental weathering was quantified in three different ways, described below.

WEIGHT LOSS

Weight loss was determined as the percentage difference between the original specimen mass and the mass of the retained portion, where the retained portion is defined as the total of any individual fragments exceeding 10% of the initial specimen dry mass. This was to avoid the distortion which can sometimes occur when the retained portion refers only to the single largest remaining piece (Nicholson and Nicholson 2000). Measurement of weight loss was accurate to ±0.1%.

FRACTURE DENSITY (F_D)

Fracture Density is a measure of the total surface area of fractures (mm^2) per unit volume of rock (mm^3) and reflects the amount of in situ breakdown. This contrasts with weight loss measurement in that fragments of material which have become detached from the main specimen are excluded from the measurement. Fracture density can be determined from simple macro-analysis of a cylindrical rock specimen. The method is based on stereological principles, enabling interpretation of three-dimensional objects, in this case fractures, on the basis of two-dimensional observations. Fractures are assumed to be obloid in three-dimensional form (ie penny shaped in plan and elliptical in cross section). The surface area to volume ratio (Sv) for planes in a given volume of material can be determined from the relationship $2P_L$, where P_L is the number of point intersections (P) per unit length ($_L$) of grid line (Underwood 1970). This equation ($Sv = 2P_L$) was

originally derived by Saltykov in 1945 and has been re-derived on a number of occasions since (see Underwood 1970 for a full review). The equation is valid for isolated and networked continuous and discontinuous surfaces and is normally used to evaluate the density of surfaces in space by counting point intersections on grid lines drawn on section planes through the medium.

In this case, the method of point counting has been modified (i) to suit the cylindrical form of the rock specimens used (100mm x 50mm diameter) and (ii) to enable non-destructive monitoring throughout experimental weathering. A standard grid was superimposed on the surface of each specimen as indicated by the grey lines in Figure 1: Four equi-distant, axial grid lines were established around the circumference of the specimen and five diametral grid lines were established along its length. The latter were spaced such that the top and bottom lines were 10mm from the edge of the specimen, with intermediate lines equally spaced between. A count was made of the number of point intersections (P) of all fractures visible to the naked eye, and the total length of grid ($_L$) measured with a calliper to an accuracy of 0.01mm, enabling Sv to be determined from $2P_L$. Because in this case the quantity Sv specifically refers to the surface area of fractures in a given volume, it is termed Fracture Density (F_D) hereafter.

Since one of the assumptions in the relationship $F_D = 2P_L$ is that fractures are circular in plan, it is possible to determine an index of mean fracture length (F_L). If F_D represents the *total* surface area of fractures per unit volume of rock ($_V$), then:

$$F_D = \frac{F\pi r^2}{V} = 2P_L \qquad (1)$$

(after Peacock et al 1994a and b) where F = the number of fractures counted, and πr^2 = the mean surface area of fracture planes, and:

Mean fracture surface area $\overline{S} = \frac{(F_D * v)}{F}$ (2)

An index of fracture length (F_L), representing the mean *diameter* of circular fractures, can then be found from:

$$F_L = 2 * \left(\sqrt{\frac{\overline{S}}{\pi}} \right) \quad (3)$$

This quantity may be useful for comparison with other methods of determining fracture length (eg Hall 1986; Tharp 1987).

Potential sources of error in Fracture Density measurement

Measurement scale: The stereological basis upon which the technique has been derived works primarily for objects viewed at the microscopic scale. However, there are good reasons for expecting that fracture density obtained at one scale will be comparable with that obtained at other orders of magnitude and an example of this is discussed in Nicholson (2000). The scale of measurement might also influence the form of fractures which can be represented by the quantity because in line with common convention in fracture mechanics, the derivation of Sv assumes an oblate, spheroidal form for microcracks. This is unlikely to be strictly valid for macroscale fractures, which sometimes assume complicated shapes and have very high aspect ratios.

Fracture length: The size of grid squares used is such that some small cracks avoid intersection and thus are 'missed' in point counting. This is counteracted in part by the fact that small fractures which do intersect with the grid tend to lead to over-estimation of F_D. Large fractures, in contrast, tend to produce under-estimates of F_D.

Stereological basis: Stereological analysis is designed for observation of two-dimensional objects in a three-dimensional media using single and serial sections through that media, or by utilising multiple visual angles or projections of it (Underwood 1970). In this case, sectioning of specimens was inappropriate for a non-destructive monitoring technique. In effect, the grid used represents serial projections on the surface of a three-dimensional medium incorporating axial and diametral (orthogonal) transects.

Classification of Fracture Density

On the basis of some field measurements of fracture intensity, Fookes and Denness (1969) produced a classification scheme of fracture intensity classes with units m^2/m^3. If the units are transposed to mm^2/mm^3 the range and distribution of fracture intensities measured actually match the theoretically derived laboratory Fracture Densities extremely well. This suggests repetition of fracture patterns at all scales. Accordingly, a modified version of the classification is presented in Figure 2 with units $x10^{-3}$ mm^2/mm^3 together with illustrations of specimens representative of each class. The classification aids judgement as to whether a particular F_D value is 'high' or 'low'.

ULTRASONIC PULSE PROPAGATION VELOCITY

Velocity indices

Because sonic wave propagation velocity in rock is dependent on a wide range of rock properties its use as an indicator of durability has long been recognised (eg Fahey and Gowan 1979). The technique is non-destructive and has the potential to detect deterioration of rock properties even where there is no visible evidence available (Goudie 1999). This provides an additional facet of observation over and above that which is obtained from weight loss and fracture density. Rather than simply compare pre and post-test pulse velocity, which is difficult to interpret, a number of

velocity indices have been proposed. Onodera (1963) proposed a Fracture Index, defined as the ratio of P-wave velocity in the rock mass to P-wave velocity in intact material. Deere at al (1967) later showed that:

$$\left(\frac{V_f}{V_l}\right)^2 = RQD \tag{4}$$

where V_f is in situ (ie measured in the field) P-wave velocity, V_l is intact (ie measured in the laboratory) P-wave velocity and RQD is Rock Quality Designation. This relation is known as the Velocity Index. Work by Sjϕgren et al (1979) on igneous and metamorphic rocks also established a good correlation between P-wave velocity and fracturing, but in some cases found that rock mass quality was better expressed by using both compressional and shear wave velocity. Other authors (eg Cratchley et al 1972) have been unable to find convincing relationships between sonic velocity and degree of fracturing and some would argue that correlation between the two is more complex than first thought (Crampin 1981).

In 1976, Fourmaintreaux proposed a Quality Index (IQ), defined as the ratio of the theoretical velocity of the unaltered rock to actual velocity:

$$IQ = \frac{Vp}{Vp_o} * 100 \tag{5}$$

where Vp is the *measured* P-wave velocity, and Vp_o is the *calculated* P-wave velocity based on the theoretical velocities of individual mineral constituents. Thus, IQ indicates in situ alteration of mineral constituents and cementing material from their unaltered state, together with rock porosity. A modification of this index (IQ_d) is to consider the ratio of the P-wave velocity measured prior to durability testing (Vp_{init}) and after *n* cycles of testing (VP_n):

$$IQ_d = \left(1 - \frac{Vp_n}{Vp_{init}}\right) * 100 \quad (6)$$

Thus IQ_d gives an indication of the amount of rock deterioration induced by experimental weathering. If used to compare deterioration in rocks with similar values for Vp_{init}, this index provides a simple and useful tool for comparative analysis. However, in rocks with widely dissimilar Vp_{init} values reduction in wave propagation velocity due to deterioration is not directly comparable in absolute terms. This is because, when a fracture is introduced into a rock which is relatively dense and has a high Quality Index, the absolute reduction in velocity is much greater than it would be if an identical fracture were introduced into a much less dense rock with a low Quality Index. This reflects the fact that the amount of change in velocity due to deterioration is a function of the pre-weathering state of the rock (ie in terms of fracture state and porosity). The net effect of this is that, although IQ_d can be usefully used to compare specimens from the same general source, it should not be used to compare rocks with widely dissimilar pre-weathering velocity values.

Fracture porosity

In an attempt to overcome this inadequacy, an Index of Fracture Porosity (IF_p) is proposed here. McDowell (1993) presents a time average formula to illustrate the way in which fractures influence wave propagation through a rock mass:

$$\frac{L}{Vp_1} = \frac{nw}{Vp_2} + \frac{(L - nw)}{Vp_3} \quad (7)$$

where L = length of direct wave path (m); n = number of fractures; w = mean width of fractures (m); Vp_1 = P-wave velocity of the bulk rock mass (ie rock material *and* fracture infill); Vp_2 = P-wave velocity of joint infill only; and Vp_3 = P-wave velocity of intact rock material only. For

instance, an intact rock mass has a measured velocity (Vp_3) of 4000ms^{-1}. Into this rock mass, 10 air-filled fractures are introduced (Vp_2 = 330ms^{-1}), each with an aperture of 0.05m (w). The length of the direct wave path is 20m. Using equation (7), the predicted velocity of the rock mass including fractures (Vp_1) will be 3130ms^{-1}. If the fractures had been filled with water (Vp_2 = 1450ms^{-1}), the resulting Vp_1 value would have been 3840ms^{-1}, indicating that there is a considerably greater attenuation for air-filled fractures than for water-filled fractures.

If the terms in equation (7) are modified such that $Vp_1 = Vp_n$ (pulse velocity after 'n' cycles of weathering); $Vp_2 = Vp_{air}$ (velocity of air infill); and $Vp_3 = Vp_{init}$ (initial, or pre-test velocity), then the equation can be re-written to determine the total volume of new fracture porosity introduced as a result of experimental weathering. Since the number of fractures introduced to the rock specimen is unknown in this context, the value for n is taken to be one and can, therefore, be disregarded, thus nw becomes w:

$$w = \frac{L\, Vp_{air}(Vp_{init} - Vp_n)}{Vp_n(Vp_{init} - Vp_{air})} \tag{8}$$

The term w then, represents the width of one, or several proportionately smaller, parallel, hypothetical fractures lying perpendicular to the direction of wave travel (across the diameter of the specimen). Since Vp_{init} reflects the inherent porosity and fracture state of the rock prior to experimental weathering, w *only* reflects *new void* introduced to the specimen as a direct result of experimental weathering. If it is also assumed that any hypothetical fracture is planar and that it fully transects a cylindrical core specimen, it is possible to calculate an absolute fracture volume, though ideally the Index of Fracture Porosity (IF_p) should be described as a percentage of specimen length.

To illustrate its use in a hypothetical example, the Vp_{init} value of a rock specimen of length 0.1m (L) is 3285ms^{-1}. Following 20 cycles of freezing and thawing a Vp_{20} value of 2915ms^{-1} is recorded. Since all velocity measurements in this research are undertaken on oven dried specimens, it is assumed any void is air-filled, and thus Vp_{air} is 330ms^{-1}. The value of w is calculated as 0.00142m. If the specimen length (L) is 100mm, IF_p is found from:

$$IF_p = \frac{w}{Specimen length(mm)} = \frac{1.42mm}{100mm} * 100 = 1.42\% \quad (9)$$

Thus, the Index of Fracture Porosity represents the aggregate percentage volume of new voids introduced into a rock as a result of induced deterioration. This new void volume might be represented by a single fracture, or more likely, by a number of proportionately smaller fractures, microcracks and pores. Since it is unlikely that all induced fractures will actually lie perpendicular to the axis of wave generation the index value should only be regarded as a comparative indicator of induced fracture porosity. Because of the nature and direction of wave movement, the Index of Fracture Porosity only applies to compression wave velocity.

To illustrate the fact that the Index of Fracture Porosity takes account of the pre-test condition of the rock, an example is described here and compared with IQ_d calculations obtained. Two contrasting rock specimens of length 100mm are subjected to experimental weathering. One is a weak, low density material with a pre-test P-wave velocity of 2500ms^{-1}, the other is a much denser, more competent material with a pre-test P-wave velocity of 6000ms^{-1}. Following experimental weathering, the corresponding velocities are reduced to 1880 and 3230ms^{-1} respectively, but in both cases, the calculated increase in fracture porosity (IF_p) is identical at 5%. In other words, the calculated amount of new void induced in the two rocks is identical, but the corresponding IQ_d values are 25% and 46% respectively. Nicholson (2000) contains results and

discussion of a comparison of fracture porosity (IFp) with pre and post-weathering porosity measured using other non-destructive (water saturation) and destructive (mercury impregnation) techniques.

Dynamic modulus of elasticity

Measurements of sonic velocity are increasingly being used to determine the dynamic modulus of elasticity (E_{dyn}) (after ASTM 1990):

$$E_{dyn} = \frac{\left[\rho Vs^2\left(3Vp^2 - 4Vs^2\right)\right]}{Vp^2 - Vs^2} \quad (10)$$

Where ρ = rock density in kg/m^3, E_{dyn} is given in Gpa, and Vs is shear-wave velocity.

E_{dyn} can also be found from Vp and ν (Poisson's Ratio), but this requires estimating a value for ν which can lead to significant inaccuracies (McDowell 1993). The percentage change in E_{dyn} can then be used as an alternative indicator of durability to IF_p. While the Index of Fracture Porosity, derived only from P-wave velocity, provides a useful indicator of the amount of void introduced into the rock due to weathering, percentage change in E_{dyn}, based on P- and S-wave velocity and rock dry density, reflects the deterioration in elastic properties and the capacity of the rock for lateral as well as axial strain. The two indices are inverse and approximately proportional. Plots of temporal change in IF_p due to weathering tend to be somewhat erratic compared to measurements of the change in E_{dyn}, and there is commonly more variation between specimens of the same rock. This is partly because E_{dyn} is a more contrived index, being based on three input variables, whereas IF_p is based on a single parameter. This means that IF_p is more susceptible to erroneous results introduced due to the size, form or location of air-filled voids. So although change in E_{dyn} enables easier interpretation of overall trends, because of its greater sensitivity IF_p

provides greater scope for detailed interpretation of processes acting within a specimen and highlights differences between individual specimens taken from the same sample.

Pulse velocity measurement method

Acoustic wave propagation velocity can be determined from both bar resonance and ultrasonic pulse methods (ISRM 1978). The latter was used throughout the experimental work reported herein. In this, a source piezoelectric transducer transmits a pulse through the axis of a specimen to a receiving transducer. Both P- and S-wave transducers were centred at a frequency of 29kHz with a usable range of 18 to 65kHz, and were housed in a steel casing to reduce any stray electromagnetic field. An Oyo pulse generator unit, model 5217A, was used to drive the transmitting transducer, providing a 500V amplitude 10μs pulse, repeated at 64 or 128 cycles per second. An Oyo Sonicviewer oscilloscope was used to measure the pulse travel time, and was powered with a 12v battery and charging unit (Figure 3).

The bottom of the rock specimen was placed on the receiving transducer with the transmitting transducer placed at the other end. Good coupling was ensured by adding a 6.6kg weight, giving an approximate normal stress of 34kPa, or 0.034N/mm^2. Vaseline coating of transducer platens was also used to improve coupling for measurements of Vp in accordance with manufacturers' advice. The apparatus was set up on a firm, flat surface.

Prior to measuring sonic velocity, oven-dried specimens were cooled at room temperature and tested within one hour to reduce the possible effect of moisture uptake from the atmosphere. Pulse travel time was determined from the mean of a minimum of three measurements of each

specimen, using more if necessary to achieve greater consistency of readings. Travel time was defined following manufacturers' recommendations, in which P-wave velocity was based on the 'first break', and S-wave velocity was based on phase difference. The first phase was determined for S-wave velocity through the rock specimen, and the second phase was based on a standard first peak for the coupled S-wave transducers.

Propagation velocity was then determined from:

$$Vp = \frac{L}{t * 10^{-6}} \text{ m sec}^{-1} \quad (11)$$

Where L is the length of the specimen (m) and t is the transit time of the pulse (μs).

For measurement of ultrasonic pulse velocity, it is necessary that specimens be effectively infinite in length in comparison to the wavelength of the generated pulse (ISRM 1978). This requires consideration of the pulse travel distance in relation to mean grain size, and the ratio of specimen diameter to pulse wavelength (ISRM 1978; ASTM 1990; Blair 1990; Siggins 1993). For all of the specimens referred to in this paper, these criteria are satisfied (Nicholson 2000).

Measurement accuracy and potential sources of error

Five potential sources of error in the measurement of acoustic wave velocities in stone weathering studies were identified by Murphy et al (1996): (a) intra-specimen variation (ie repeatability); (b) inter-specimen variation; (c) specimen geometry; (d) moisture content; (e) applied pressure. The potential effects of these and other factors are considered below:

Repeatability: The vast majority of travel time readings fell within an accuracy of ±0.5% which is comparable to that achieved by Allison (1988) using the Grindosonic resonance bar technique.

Inter-specimen variation: Variation between specimens is expected even when they are derived from the same original block because even minor variations in weathering, microcrack density and porosity affect wave propagation. In fact specimen variation was deliberately incorporated into this experimental work in order to enable investigation and interpretation of anomalies.

Specimen geometry: All specimens were cut to an identical geometry.

Moisture content: While S-wave velocity appears to be little affected, P-wave velocity generally increases with increasing moisture content (McDowell 1993). To remove any potential source of error associated with moisture content, all specimens were oven-dried and cooled at room temperature prior to measurements being taken. To determine the potential for moisture uptake from the atmosphere, a set of control specimens was repeatedly measured over several hours on a humid day and some specimen surfaces were also variously wetted. The amount of moisture uptake, if any, was insufficient to cause any significant change in travel time readings.

Applied pressure: A standard normal load of 34kPa was applied for all measurements to achieve good coupling with transducers. The amount of load applied was insufficient to cause acoustic closure (New 1976; New and West 1980).

Other possible sources of error: Cracks which form parallel to the core axis will tend to produce greater acoustic attenuation than those which form perpendicular to it. This might also occur

where the generated pulse intersects isolated cavities or other significant anomalies in the rock. In this experimental work the problem has been limited as much as possible by preparing specimens with the dominant alignment of bedding and other linear features perpendicular to the core axis. Furthermore, measurements were always taken with specimens oriented identically with transducers positions fixed, to avoid any orientation bias.

DISCUSSION OF SOME RESULTS

The results of temporal variations in weight loss, fracture density and fracture porosity are shown in Figure 4 for a Triassic micaceous sandstone (St Bees formation, west Cumbria) subjected to simulated freeze-thaw. Negligible weight loss occurred and the trends for individual specimens appear erratic only because the values are close to the margin of error of the measurement method. Four out of five of the five specimens tested showed an initial increase in F_D followed by a tailing off, although F_D values are generally low. In contrast to weight loss and fracture density, IF_p was relatively high, probably indicative of an increase in the amount of air-filled void present internally. These results indicate that internal modifications may have occurred despite little visible evidence of such. This is supported by pre and post-test measurement of porosity and pore size distribution which indicate an increase in both total void space and the proportion of large pores. This illustrates how indices which focus on macro-scale, visible breakdown may fail to reveal deterioration which occurs either internally, or at the microscale. The results also provide a good example of poor agreement between different deterioration indicators. Had breakdown been assessed on the basis of weight loss alone the interpretation of rock susceptibility to weathering and understanding of the processes operating would have been incomplete.

Two sets of results from a salt weathering test illustrate further aspects of the relative merits of different deterioration indicators. Results for a Permian magnesian limestone (west Yorkshire) are shown in Figure 5. These show that initially, a weight *gain* occurred, probably indicating pore infilling by crystallised salt deposition. Weight *loss* occurred subsequently due to the detachment of substantial fragments of material. In the remaining intact portion of the specimen, change in F_D indicates that a steady increase in *in situ* fracturing occurred. An inverse and proportionate reduction in IF_p also occurred which indicates an increase in pulse propagation velocity. Like the initial *gain* in weight, this might also suggest infilling of air-filled voids with salt deposits. These results are a good example of how different facets of information indicated by the three measurements can enable a more holistic interpretation of the processes acting. In this case they may aid understanding of the potential influence of experimental design on results.

In a further salt weathering test conducted in a hard Yorkshire chalk (Figure 6), a steady increase in weight occurred, again, likely to be the result of salt deposition. These specimens also developed a dense network of angular, hairline cracks on the surface of specimens. However, in contrast to the magnesian limestone, this rock showed an increase in IF_p. This indicates greater pulse attenuation due to an increase in air-filled voids. So, despite evidence of salt deposition in pores from the weight loss data, a considerable amount of new void must nevertheless have been introduced, reflected also by the increase in F_D. The specimen showing a particularly high IFp after 5 cycles probably reflects the development, after two cycles, of a very wide, persistent crack running transversely across the rock cylinder.

A laminated Coal Measures siltstone subjected to repeated cycles of wetting and drying (Figure 7) showed a modest weight loss for most specimens, but very high values for F_D and IF_p. This is

helpful in indicating the style of breakdown for this particular rock. In this case, the rock had a high susceptibility to in situ breakdown and comparative resistance to detachment. In a contrasting example (results not shown here) a coarse-grained sandstone from the Millstone Grit showed a moderate weight loss due to the detachment of individual grains, but there was no indication of surface fracturing or of internal modification.

CONCLUSIONS

Different measurements of rock breakdown reflect different facets of the processes involved. Weight loss, for instance, reflects susceptibility to detachment of grains or fragments. An increase in fracture density reflects susceptibility to in situ rupture. The Index of Fracture Porosity reflects changes in the amount of air-filled space, commonly indicating internal, and thus hidden, modification. These measurements made on the same specimen may not indicate identical trends because they reflect different aspects of breakdown. Experimental rock weathering studies would benefit from the use of complementary, multiple breakdown indicators to enable a more complete understanding of the processes operating (including any unwanted effects of experimental design) and the relative importance of different modes of breakdown.

REFERENCES

ALLISON, R. J. A non-destructive method of determining rock strength. *Earth Surface Processes and Landforms* 13, 729-736. (1988).

ALLISON, R. J. Developments in a non-destructive method of determining rock strength. *Earth Surface Processes and Landforms* 15, 571-577. (1990).

ASTM (American Society For Testing Materials) C2845-90. *Standard Test Method for Laboratory Determination of Pulse Velocities and Ultrasonic Elastic Constants of Rock.* Philadelphia. (1990).

BLAIR, D. P. The longitudinal pulse velocity in finite cylindrical cores. *Journal Acoustic Society America* 88 (2), 1123-1131. (1990).

CRAMPIN, S. A review of wave motion in anisotropic and cracked elastic media. *Wave Motion* 3, 343-391. (1981).

CRATCHLEY, C. R., GRAINGER, P., McCANN, D. M. and SMITH, D. I. Some applications of geophysical techniques in engineering geology with special reference to the Foyers Hydroelectric scheme. *In: Proceedings of the 24th International Geological Congress*, Montreal, section 13, 163-175. (1972).

DEERE, D. U., HENDRON, A. J. Jr., PATTON, F. D. and CORDING, E. J. Design of surface and near-surface construction in rock. *In:* C. Fairhurst (ed.) *Proceedings 8th U. S. Symposium Rock Mechanics*, Minneapolis, MN, Port City Press, Baltimore MD, 237-302. (1967).

FAHEY, B. D. and GOWAN, R. J. Application of the sonic test to experimental freeze-thaw studies in geomorphic research. *Arctic and Alpine Research* 11, 253-260. (1979).

FOOKES, P. G. and DENNESS, B. Observational studies of fissure patterns in Cretaceous sediments of south-east England. *Geotechnique* 19 (4), 453-477. (1969).

FOURMAINTREAUX, D. Characterisation of rocks: laboratory tests. *In:* M. Panet (ed.) *Mecanique des Roches Appliquee aux Ouvrages du Genie Civil*, Ecole Nationale des Ponts et Chausees, Paris. (1976).

GOUDIE, A. Further experimental investigation of rock weathering by salt and other mechanical processes, *Zeitschrift fur Geomorphologie Supplementband* 21, 1-12. (1974).

GOUDIE, A. S. Experimental salt weathering of limestones in relation to rock properties. *Earth Surface Processes and Landforms* 24, 715-724. (1999).

HALL, K. J. The utilization of the stress intensity factor (K_{IC}) in a model for rock fracture during freezing: An example from Signy Island, the Maritime Antarctic. *British Antarctic Survey Bulletin* 72, 53-60. (1986).

ISRM. (International Society for Rock Mechanics, Commission on Standardisation of Laboratory and Field Tests) Suggested methods for determining sound velocity. *International Journal Rock Mechanics Mining Science* 15, 53-58. (1978).

JERWOOD, L. C., ROBINSON, D. A. and WILLIAMS, R. B. G. Experimental frost and salt weathering of chalk - I. *Earth Surface Processes and Landforms* 15, 611-624. (1990a).

JERWOOD, L. C., ROBINSON, D. A. and WILLIAMS, R. B. G. Experimental frost and salt weathering of chalk - II. *Earth Surface Processes and Landforms* 15, 699-708. (1990b).

McDOWELL, P. Seismic investigation for rock engineering. *In:* J. A. Hudson (ed.) *Comprehensive Rock Engineering: Principles, Practice and Projects* 3, Pergamon Press, Oxford, 619-634. (1993).

MURPHY, W. and INKPEN, R. J. Alteration of geotechnical properties of Portland limestone and Monks Park limestone under simulated weathering. *In:* J. Riederer (ed.) *Deterioration and Conservation of Stone*, Proceedings 8th International Congress, Berlin, volume 2, Moller, 739-750. (1996).

MURPHY, W., SMITH, J. D. and INKPEN, R. J. Errors associated with determining P and S acoustic wave velocities for stone weathering studies. *In*: B. J. Smith and P. A. Warke (eds) *Processes of Urban Stone Decay*, Donhead Publishing Ltd, 228-244. (1996).

NEW, B. M. Ultrasonic wave propagation in discontinuous rock. *Transport and Road Research Laboratory,* Report LR 720, Department of the Environment. (1976).

NEW, B. M. and WEST, G. The transmission of compressional waves in jointed rock. *Engineering Geology* 15, 151-161. (1980).

NICHOLSON, D. T. *Deterioration of Excavated Rockslopes: Mechanisms, Morphology and Assessment*. PhD Thesis, University of Leeds. (2000).

NICHOLSON, D. T. and NICHOLSON, F. H. Physical deterioration of sedimentary rocks subjected to experimental freezing and thawing. *Earth Surface Processes and Landforms* 25, 1295-1307. (2000).

NICHOLSON, D, T. Pore properties as indicators of breakdown mechanisms in experimentally weathered limestones. *Earth Surface Processes and Landforms* 26. 819-838 (2001).

ONODERA, T. F. Dynamic investigation of foundation rock in situ. *In:* C. Fairhurst (ed.) *Proceedings of the 5th US Symposium on Rock Mechanics*, Minneapolis, MN, Peragamon Press, Oxford. (1963).

PEACOCK, S., McCANN, C., SOUTHCOTT, J. and ASTIN, T. R. Experimental measurements of seismic attenuation in microfractured sedimentary rock. *Geophysics* 59 (9), 1342-1351. (1994a).

PEACOCK, S., McCANN, C., SOUTHCOTT, J. and ASTIN, T. R. Seismic velocities in fractured rocks: an experimental verification of Hudson's theory. *Geophysical Prospecting* 42 (1), 27-80. (1994b).

SIGGINS, A. F. Dynamic elastic tests for rock engineering. *In:* J. A. Hudson (ed.) *Comprehensive Rock Engineering: Principles, Practice and Projects* 3, Pergamon Press, Oxford, 601-618. (1993).

SJϕGREN, B. A., OFTHUS, A. and SANDBERG, J. Seismic classification of rock mass qualities. *Geophysical Prospecting* 27, 409-442. (1979).

SWANTESSON, J. Experimental weathering studies of Swedish rocks. *Geografiska Annaler* 67A (1-2), 115-118. (1985).

THARP, T.M. Conditions for crack propagation by frost wedging. *Geological Society America Bulletin* 99 (1), 94-102. (1987).

TOROK, A., GALOS, M. and KOSCANYI-KOPECSKO, K. Experimental weathering of rhyolite tuff building stones. Abstract in: *Weathering 2000*, Queens University Belfast, June 2000, p45. (2000).

TUGRUL, A. Change in pore size distribution due to weathering of basalts and its engineering significance. *In:* P. G. Marinos, G. C. Koukis, G. C. Tsiambaos and G. C. Stournara (eds) *Engineering Geology and the Environment*, Volume 1, Balkema, Rotterdam, 419-424. (1997).

UNDERWOOD, E. E. *Quantitative Stereology*. Addison-Wesley Publishing Co. Reading. (1970).

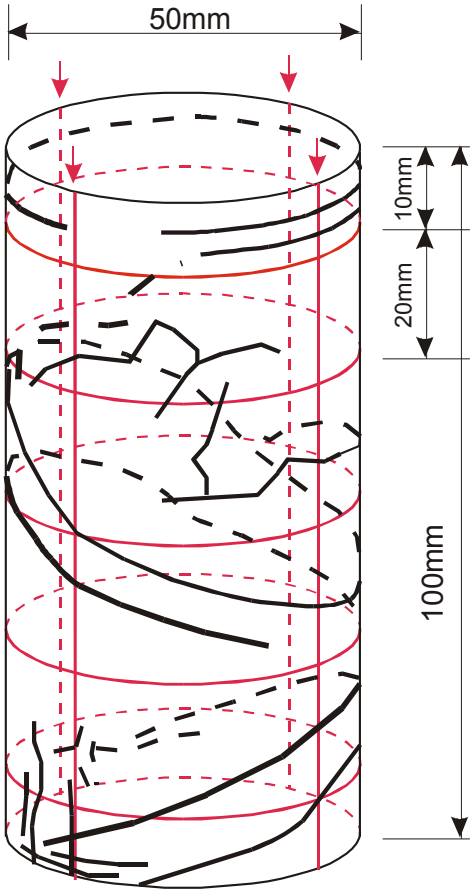

Figure 1 Grid superimposed on rock specimens for point counting of intersections

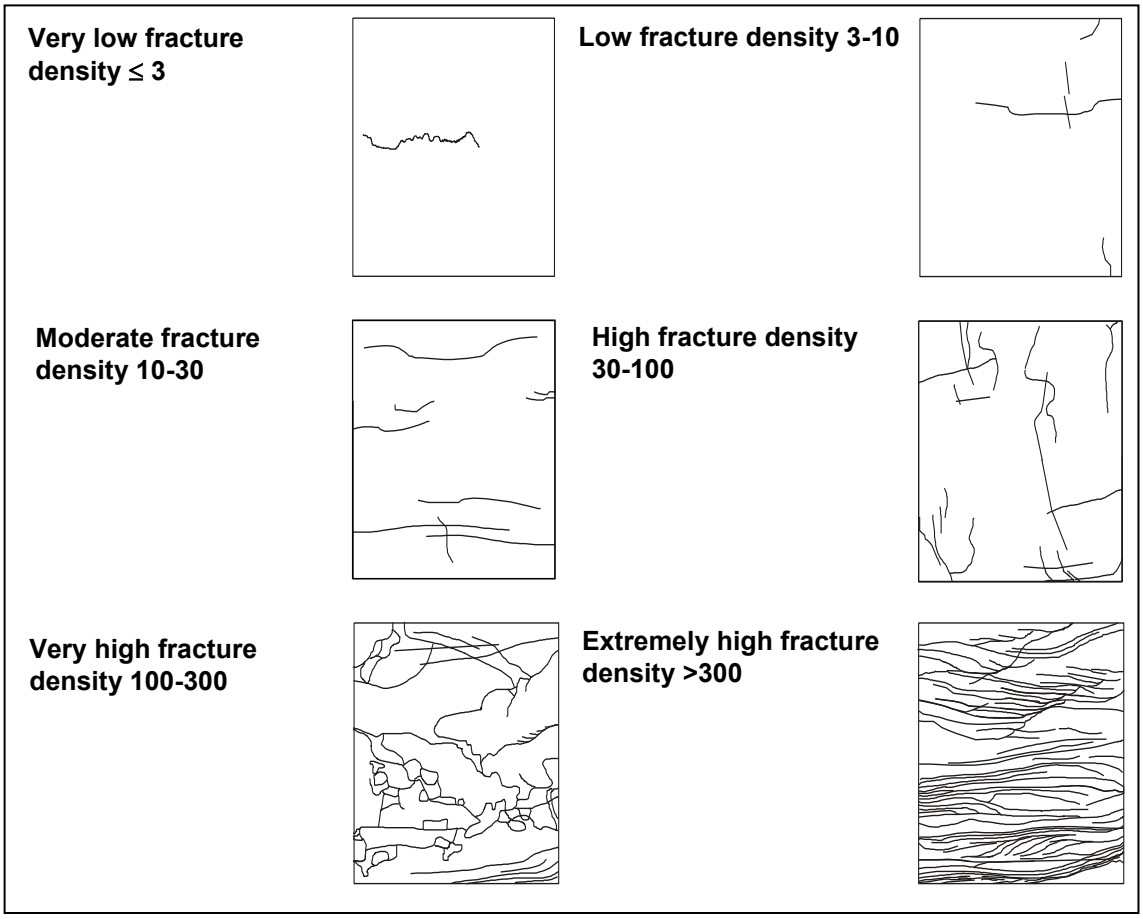

Figure 2 Classification of Fracture Density (units are $x10^{-3}$ mm^2/mm^3)
Sketches are indicative Fracture Densities based on the specimens tested

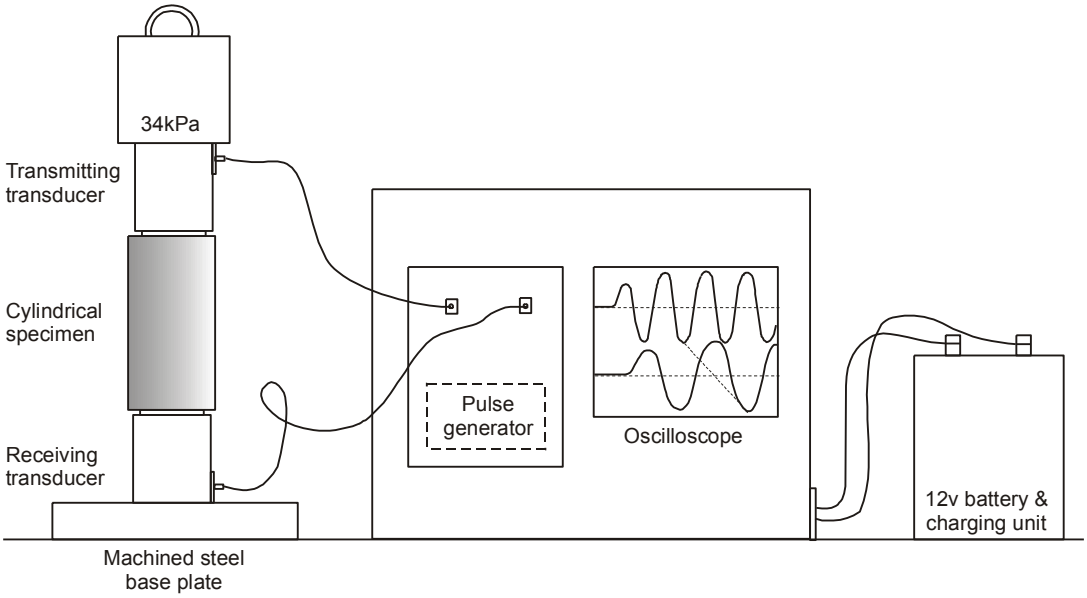

Figure 3 Schematic representation of ultrasonic pulse velocity measurement apparatus

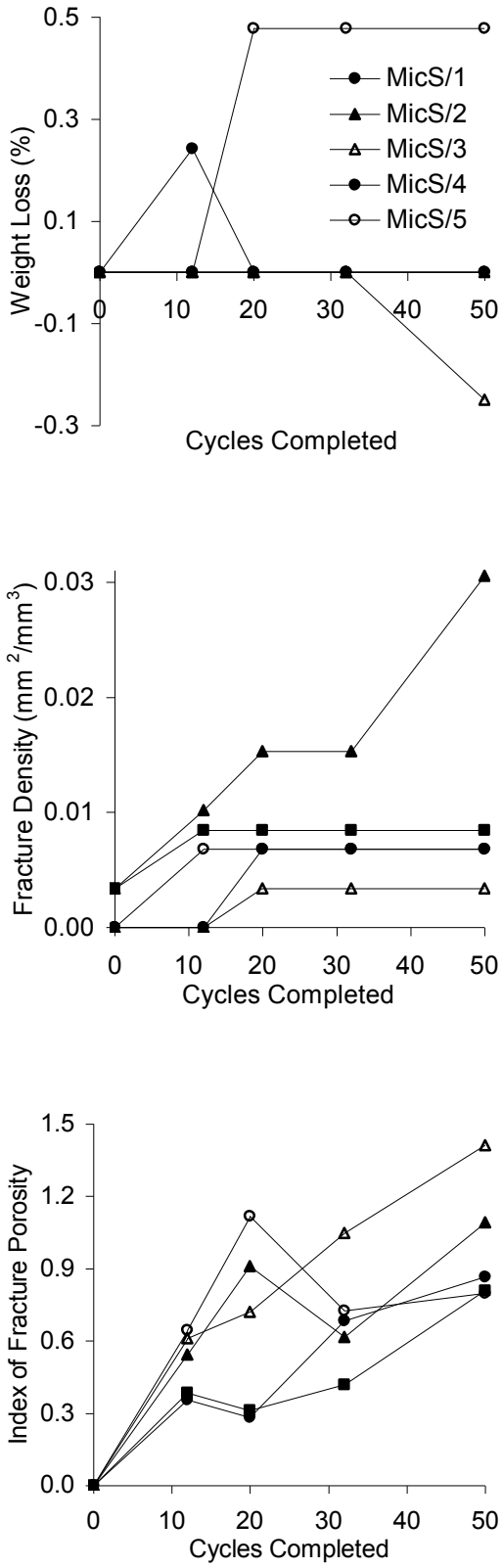

Figure 4 Deterioration indicators for the micaceous sandstone after 50 cycles of freeze-thaw

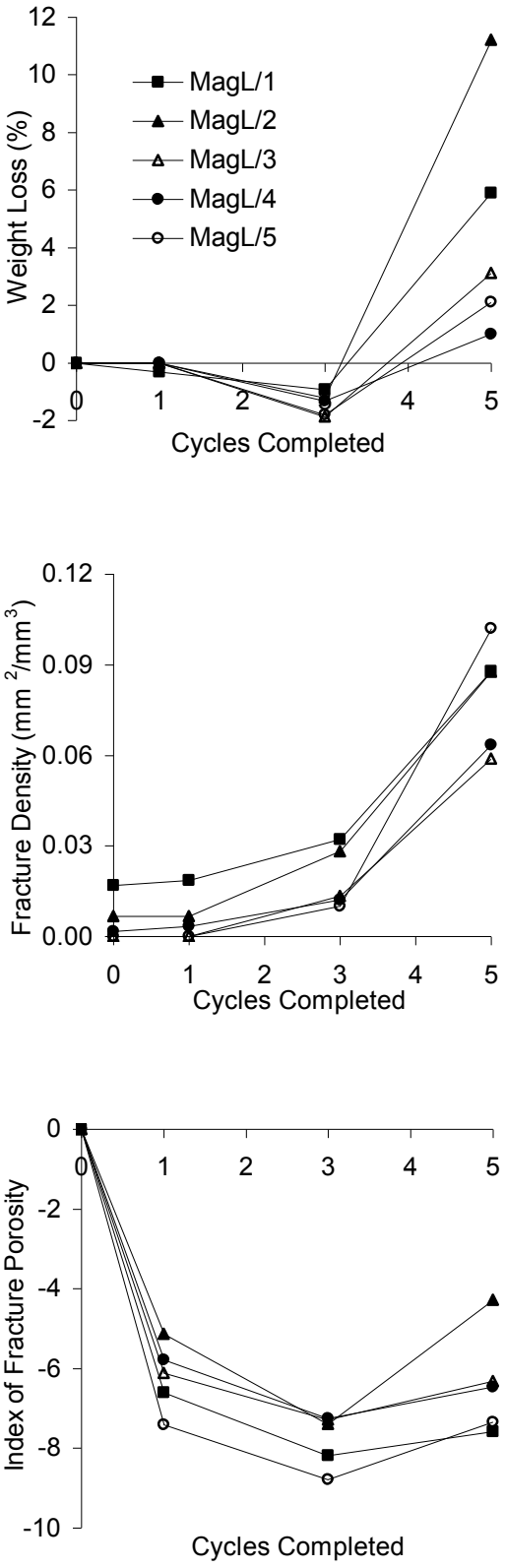

Figure 5 Deterioration indicators for the magnesian limestone after 5 cycles of salt weathering

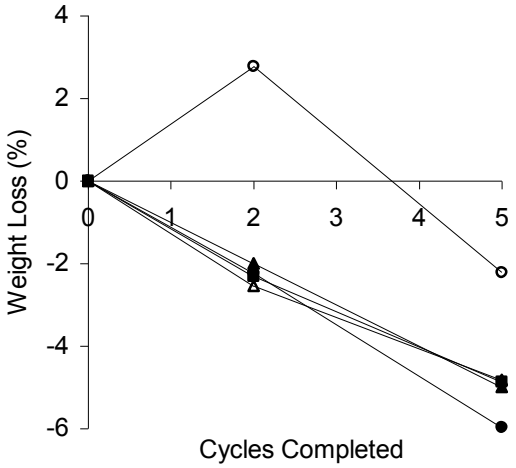

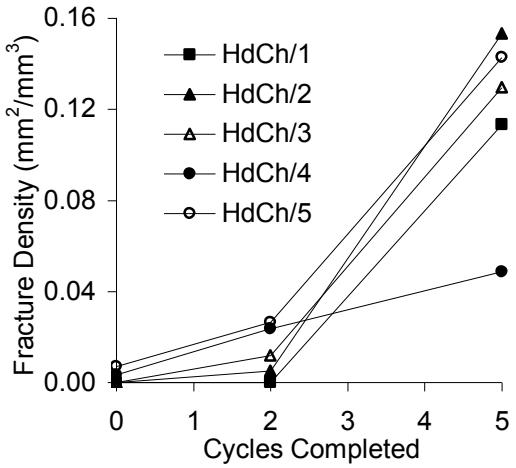

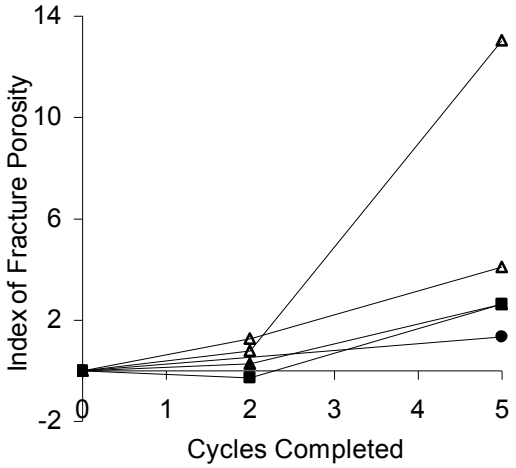

Figure 6 Deterioration indicators for the hard chalk after 5 cycles of salt weathering

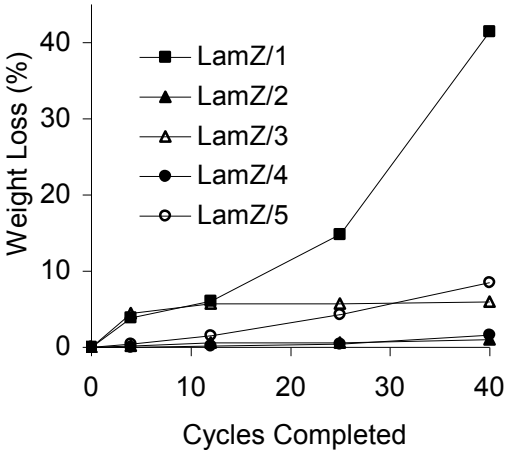

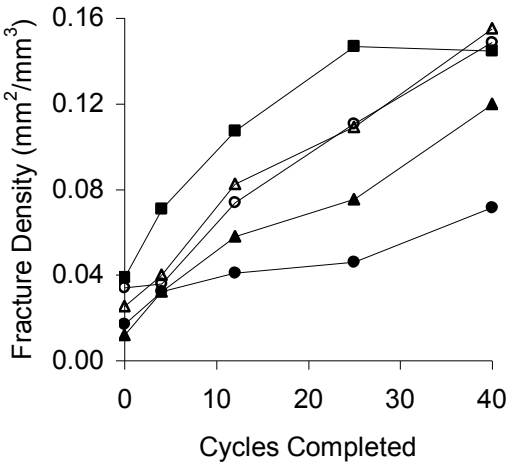

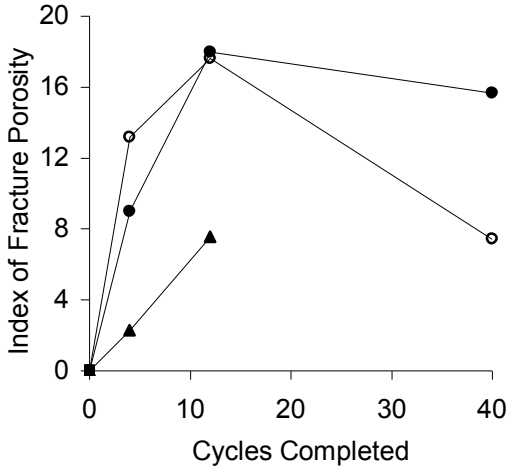

Figure 7 Deterioration indicators for the laminated siltstone after 40 cycles of wetting and drying